

## DOCUMENT CONTROL DATA - R &amp; D

(Security classification of title, body of abstract and indexing annotation must be entered when the overall report is classified)

1. ORIGINATING ACTIVITY (Corporate author)		2a. REPORT SECURITY CLASSIFICATION	
Naval Research Laboratory Washington, D.C. 20390		Unclassified	
		2b. GROUP	
3. REPORT TITLE			
CHARACTERIZATION OF TIG WELDS IN 12-5-3 MARAGING STEEL PLATE WITH APPLICATION OF A NEW SCALING METHOD FOR $K_{Ic}$ PLASTICITY CORRECTIONS			
4. DESCRIPTIVE NOTES (Type of report and inclusive dates)			
A final report on one phase of the problem; work is continuing on other phases.			
5. AUTHOR(S) (First name, middle initial, last name)			
F. R. Stonesifer and H. L. Smith			
6. REPORT DATE		7a. TOTAL NO. OF PAGES	7b. NO. OF REFS
April 16, 1970		27	9
8a. CONTRACT OR GRANT NO.		9a. ORIGINATOR'S REPORT NUMBER(S)	
NRL Problems F01-15 and F01-03		NRL Report 7053	
b. PROJECT NO.			
NASA Contract W-11,763			
c.		9b. OTHER REPORT NO(S) (Any other numbers that may be assigned this report)	
Project RR009-03-45-540			
d.			
10. DISTRIBUTION STATEMENT			
This document has been approved for public release and sale; its distribution is unlimited.			
11. SUPPLEMENTARY NOTES		12. SPONSORING MILITARY ACTIVITY	
Also sponsored by the National Aeronautics and Space Administration		Department of the Navy (Office of Naval Research), Washington, D.C. 20360	
13. ABSTRACT			
<p>The 12Ni-5Cr-3Mo maraging steel has been found to maintain good toughness at the intermediate-to-high strength level. This report is concerned with fabricating and optimizing weld joints in the 12-5-3 maraging steel. Three weld-wire compositions, two TIG welding processes, and two heat-treating sequences were compared in all possible combinations. Welds and weld repairs were compared in tensile, impact, fracture-toughness, and metallographic evaluations. Various comparisons are presented in tables and graphs.</p> <p>These data show that the slightly increased yield strength obtained through the Big TIG welding process is more than offset by the reduced toughness. <math>K_{Ic}</math> values, obtained from the three-point bend test, showed slight advantages in using a weld wire with a lower percentage of titanium and in welding the plate in the aged condition. However, multiple weld repairs may cause as much as a 26-percent decrease in weld toughness. The greatest reduction in toughness was found in the plates that had three aging cycles: one before welding, one after welding, and the third after weld repairs had been made.</p> <p>Corrections were applied to mixed-mode fracture-toughness values in an attempt to obtain valid <math>K_{Ic}</math>, plane-strain fracture-toughness, numbers. Plasticity corrections based on <math>\Delta a = r_y = K_{Ic}^2 / 6\pi\sigma_y^2</math> were far too large for these specimens. A new scaling method based on equivalent elastic-fracture strain gave a correction independent of specimen size in accordance with the principles of fracture mechanics.</p>			

14.

KEY WORDS

LINK A

LINK B

LINK C

ROLE

WT

ROLE

WT

ROLE

WT

Fracture Toughness  
TIG welds  
Maraging steel

## CONTENTS

Abstract	ii
Problem Status	ii
Authorization	ii
SYMBOLS	iii
INTRODUCTION	1
FRACTURE-TOUGHNESS TESTS AND THEIR VALIDITY	2
TESTING PROGRAM	4
DATA AND TEST RESULTS	5
Welded Test Panels	5
Weld Repairs	14
SUMMARY AND CONCLUSIONS	20
ACKNOWLEDGMENT	21
REFERENCES	21

## ABSTRACT

The 12Ni-5Cr-3Mo maraging steel has been found to maintain good toughness at the intermediate-to-high strength level. This report is concerned with fabricating and optimizing weld joints in the 12-5-3 maraging steel. Three weld-wire compositions, two TIG welding processes, and two heat-treating sequences were compared in all possible combinations. Welds and weld repairs were compared in tensile, impact, fracture-toughness, and metallographic evaluations. Various comparisons are presented in tables and graphs.

These data show that the slightly increased yield strength obtained through the Big TIG welding process is more than offset by the reduced toughness.  $K_{Ic}$  values, obtained from the three-point bend test, showed slight advantages in using a weld wire with a lower percentage of titanium and in welding the plate in the aged condition. However, multiple weld repairs may cause as much as a 26-percent decrease in weld toughness. The greatest reduction in toughness was found in the plates that had three aging cycles: one before welding, one after welding, and the third after weld repairs had been made.

Corrections were applied to mixed-mode fracture-toughness values in an attempt to obtain valid  $K_{Ic}$ , plane-strain fracture-toughness, numbers. Plasticity corrections based on  $\Delta a = r_y = K_{Ic}^2 / 6\pi\sigma_y^2$  were far too large for these specimens. A new scaling method based on equivalent elastic-fracture strain gave a correction independent of specimen size in accordance with the principles of fracture mechanics.

## PROBLEM STATUS

This is a final report on NASA Contract W-11,763. Additional work with some change in emphasis is being continued under a different NASA contract. Part of the work on determining the validity of fracture-toughness testing was supported by ONR funds.

## AUTHORIZATION

NRL Problems F01-15 and F01-03  
NASA Contract W-11,763 and Project No. RR 009-03-45-540

Manuscript submitted January 13, 1970.

## SYMBOLS

$a$	effective length, half-length, or depth of crack according to type of specimen, $a = a_0 + \Delta a$
$a_0$	length of open crack
$\Delta a$	increment added to $a_0$ to account for plastic flowing, equal to $r_y$
$B$	plate or specimen thickness
$B'$	net $B$ for side-grooved specimens
$D$	specimen depth
$E$	Young's modulus of the material
$\mathcal{G}$	strain-energy release rate per unit area of fracture
$K$	fracture-toughness stress-intensity factor, $K = \sqrt{E\mathcal{G}/(1 - \nu^2)}$ , for plane strain
$K_I$	value of $K$ for opening mode of crack extension
$K_{Ic}$	critical plane-strain value of $K$
$L$	total span for bend-bar specimen
$L'$	moment arm, one-half of $L$ for three-point bend test
$P$	applied load
$r_y$	increment related to plastic zone size, equal to $\Delta a$
$\sigma$	applied nominal tensile stress
$\sigma_y$	yield strength of the material
$\nu$	Poisson's ratio



# CHARACTERIZATION OF TIG WELDS IN 12-5-3 MARAGING STEEL PLATE WITH APPLICATION OF A NEW SCALING METHOD FOR $K_{Ic}$ PLASTICITY CORRECTIONS

## INTRODUCTION

Design engineers are in urgent need of stronger, tougher materials to optimize pressure-vessel design and satisfy the leak-before-failure criterion which is so essential for successful space and deep ocean exploration. Each candidate material must be thoroughly evaluated before it may be considered for practical applications. Then additional tests may be required for each new application of a given material. How will a material react to a hostile environment? Will stress corrosion be a problem? At present, these questions can only be answered through a test and evaluation program.

Improved compositions, melting practices, and processing techniques have made higher strength materials a reality during the past decade. Higher strength materials are particularly attractive in today's interests, where a premium must be paid for additional weight. A structure's strength-to-weight ratio comes under close scrutiny, and deliberate over-design with use of large safety factors is no longer feasible in many instances. Material properties must be separated, defined, and accurately determined.

Unfortunately, higher strength in a material is normally accompanied by lower fracture toughness, smaller critical crack sizes, and danger of catastrophic brittle failures at stresses considerably below the yield strength of the material. All known materials contain flaws in the form of inclusions, cracks, grain boundaries, and voids; but in most cases critical-size flaws are introduced during fabrication. Welding and forming can produce both metallurgical and physical flaws as stress risers. All critical-size flaws must be detected visually or through nondestructive testing so that corrective steps may be taken. Consideration should also be given the subcritical-size flaws to insure that they will not extend to critical size during the normal useful life of the structure. In reality, the engineer must choose a relatively strong material with sufficient toughness to allow for the detection of subcritical-size flaws by nondestructive testing techniques.

The maraging class of steel is one of the first of the new family of high-strength, high-toughness materials developed during the past few years. Maraging steels were introduced about 1960 and have been improved since then through extensive research and development programs. The relatively simple heat treatment of the maraging steels is one of their major advantages. They are normally solution annealed (simultaneously austenitized and solution treated) at 1500°F and air cooled. The structure of the alloy when cooled to room temperature is that of a low-carbon, body-centered cubic martensite with a hardness of approximately Rockwell C32. The material is easily machined and formed when in this condition. High-strength properties are developed rapidly when this martensitic structure is aged at 900°F. Strengthening during aging results from complex precipitation reactions in the martensitic matrix. These properties make this class of steel particularly attractive for modern applications (1).

The 12-5-3 maraging steel (12Ni-5Cr-3Mo) was designed specifically for applications requiring optimum combinations of relatively high-yield strength and toughness. As with the earlier 18%-Ni maraging alloy, its properties are developed by a solution treatment followed by an aging cycle. It responds to a wide range of solution and aging temperatures, making it versatile and adaptable to various situations.

The 12%-Ni maraging steel is of particular interest in the 180-ksi yield-strength range. In this strength range, the material maintains good fracture-toughness characteristics, along with its relatively high yield strength, to give a good toughness-to-yield-strength ( $K_{Ic}/\sigma_y$ ) ratio (2). It is this material, 12%-Ni maraging steel in the 180-ksi yield-strength range, which has been evaluated in this study. A full chemical analysis of one heat of 12Ni-5Cr-3Mo steel is shown in Table 1.

Cyclic and burst tests on vessels both free from, and containing purposely induced, flaws have proven the capability of 12%-Ni materials for "leak-before-failure" in the cylinders with 1/2-in.-thick walls (3). This study by the Boeing Company used the gas-tungsten-arc process to produce extremely tough weldments in both air-melt and vacuum-melt plates. They found weldments in both types of plates capable of meeting the "leak-before-failure"

criterion. Boeing used a 17%-Ni filler wire but suggested that a 12%-Ni nearly matching chemistry might improve toughness and fusion characteristics. All their specimens were aged after welding.

Table 1  
Chemical Analyses of One Heat of 12Ni-5Cr-3Mo Steel

Element	Composition (wt-%)							
	Base Plate*		Weld Wires					
	HT #L50896		HT #03028		HT #09794		HT #09847	
	Vendor's Analysis	NRL's Analysis	Vendor's Analysis	NRL's Analysis	Vendor's Analysis	NRL's Analysis	Vendor's Analysis	NRL's Analysis
C	0.01	0.017	0.01	0.023	0.01	0.023	0.02	0.023
Mn	0.04	0.06	0.03	0.05	0.05	0.03	0.02	0.02
P	0.007	0.010	0.004	0.008	0.002	0.005	0.005	0.010
S	0.002	0.005	0.005	0.007	0.006	0.005	0.006	0.007
Si	0.06	0.07	0.05	0.07	0.02	0.02	0.02	0.02
Mo	3.10	3.00	3.17	2.70	2.85	2.65	3.63	3.25
Ni	12.05	11.4	12.1	11.1	16.9	15.0	18.1	16.8
Al	0.30	0.35	0.31	0.15	0.02	0.02	0.04	0.04
Cr	4.72	4.78	4.04	5.03	—	—	—	—
Ti	0.28	0.28	0.40	0.34	0.54	0.48	0.19	0.18
Co	—	—	—	—	2.26	2.20	7.47	7.72
Ca	—	—	—	—	—	—	0.02	—
Cd	—	—	0.05 (added)	—	—	—	(added)	—

\*Gas analysis of base plate: N = 21 ppm, O = 27 ppm, H = 1 ppm.

The study reported on here used the vacuum-melted 12%-Ni plate in conjunction with three weld-wire chemistries, two heat-treating sequences, and two variations in the tungsten-arc welding process. These variables are described in detail later in the report.

## FRACTURE-TOUGHNESS TESTS AND THEIR VALIDITY

The precracked, three-point-bend, bar specimen and testing method as recommended by Kies and others, (4) was adapted for this program. The specimens, as shown in Fig. 1, were notched 20% of the total bar depth and side grooved 5% of the width on both sides. The notch was then extended another 5 to 10% by cyclic bending. The total notch depth, or initial crack depth, is the total of the machined notch plus the fatigue-crack extension. This sharp crack front represents a severe natural crack situation. The modified Kies equation (5) used in the calculation of plane-strain fracture toughness may be written

$$K_I = 1.9 [1/(1 - a/D)^3 - (1 - a/D)^3]^{1/2} PL'/DB^{3/2}(B/B')^{1/2}.$$

This equation gives values within 1% of those obtained from the ASTM proposed formula over the range of a/D from 0.25 to 0.67. A comparison of the two equations has been published in the "Report of NRL Progress" (5). Since no "pop-in" is observed for materials of this class, the ultimate load was used in calculating the uncorrected  $K_{Ic}$  values. The term  $(B/B')^{1/2}$  is added to the Kies equation to compensate for the side grooves.

A valid plane-strain, fracture-toughness measurement should be independent of specimen size. There is, however, a minimum size below which general plastic yielding occurs before crack propagation. This size depends on the ratio between toughness and yield strength for the material. When the plastic zone ahead of the crack becomes large in comparison with specimen dimensions, brittle plane-strain fracture is inhibited and the calculated K values do not represent true plane-strain values.

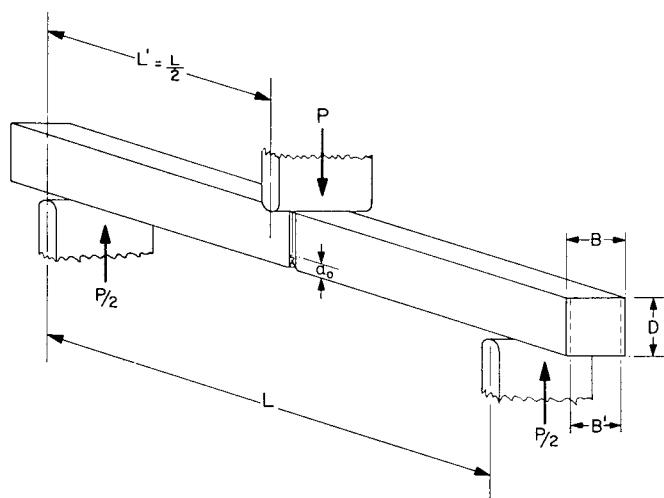


Fig. 1 – Single-edge-cracked, three-point-bend bar.

ASTM Committee E-24 has set minimum specimen size limits and recommendations for determining test validity (6). One recommendation is that no specimen dimension should be less than  $2.5 (K_{Ic}/\sigma_y)^2$ . These limits are based on results from tests on what might now be considered materials of medium toughness. The committee has not yet attempted to solve the problem for materials in which the toughness  $K_{Ic}$  ( $\text{ksi}\sqrt{\text{in.}}$ ) exceeds the tensile yield strength  $\sigma_y$  (ksi). In such cases, specimen sizes become prohibitive under the proposed recommended practice. Therefore, this proposed practice may not be practical for testing the new improved high-nickel-content materials. With these materials, the  $K_{Ic}$  ( $\text{ksi}\sqrt{\text{in.}}$ ) value may be as high as three times the yield (ksi).

A continuing effort is being made to adjust or correct values obtained from “undersized specimens” to reflect true plane-strain values. A graphical correction method, based on the Irwin plasticity correction, has been proposed (7). The graphical method provides for a convenient solution for the Irwin correction, but it neither affects the validity of the correction nor extends the range of its application. Another method based on equivalent elastic-fracture strain instead of stress (8), which we call the scaling method, appears to work better over a larger range of  $a/D$  values.

This new correction technique assumes that if the specimen had been of sufficient size, general yielding would not have occurred before crack propagation or instability. The total strain at failure would then have been completely elastic. Failure would have occurred at the load represented by the intersection of a line extended through the elastic portion of the load-vs-deflection curve and a constant strain, or deflection, line through the point of crack instability. Any crack growth prior to this point should be considered subcritical and would only contribute to the original crack length. The load value corresponding to this intersection is used in the  $K_{Ic}$  calculation. Figure 2 illustrates the method used to determine this load value. This method appears to work well for the 12%Ni material examined here; however, only a very limited number of specimens have been tested to date. (It should be noted that the material used in this particular study was 4-in.-square bar stock of 12-5-3 alloy but not from the same heat used for the data in the remainder of the report.) Figure 3 shows a comparison of the uncorrected data with values from the two correction methods. This new scaling method, based on equivalent elastic-fracture strain, was used in correcting data in this report. These corrected values should be very near to the true plane-strain fracture-toughness parameter. For this material, a bend specimen approximately 16-1/2 by 8-1/4 by 165 in. would have been necessary to meet the requirements for a valid  $K_{Ic}$  as proposed by the ASTM (6).

The plane-strain fracture-toughness parameter  $K_{Ic}$  is a material property and as such does not depend on specimen configuration or size. If the specimen is undersized, the uncorrected  $K$  obtained from the test will be for a mixed mode of plane strain and plane stress. In cases where the material is to be used in sections that are too thin to obtain true  $K_{Ic}$  values, the mixed-mode  $K$  obtained from these thin sections may actually be of more value to the design engineer than the true plane-strain  $K_{Ic}$  number. For this reason the uncorrected values have also been recorded for the 1-in. material studied.

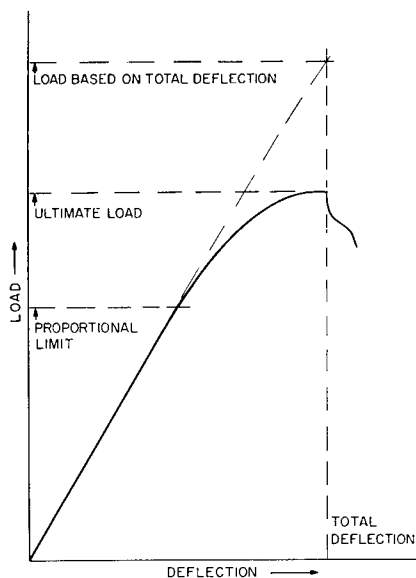


Fig. 2 - Load-deflection curve for pre-cracked  $K_{Ic}$  bend bar specimen.

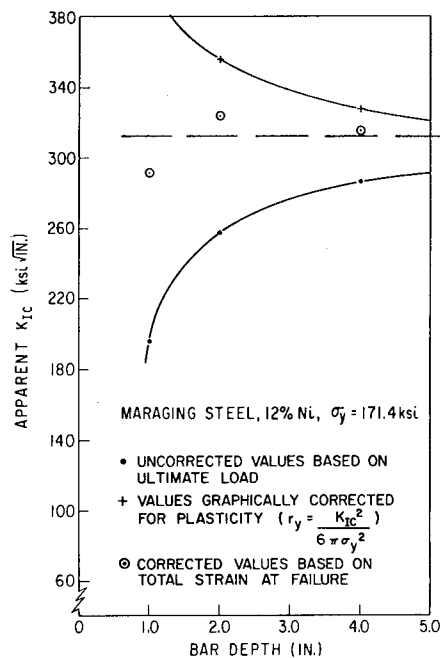


Fig. 3 - Apparent  $K_{Ic}$  vs bar depth  $D$

All  $K_{Ic}$  values in this report, both corrected and uncorrected, are listed as apparent  $K_{Ic}$ , since the tests did not meet the proposed standards set by the ASTM (6).

## TESTING PROGRAM

A testing program was set up to evaluate welding and heat-treating parameters for 12%-Ni maraging steel in the 180-ksi yield-strength range. One-inch-thick plate material was used in determining an optimum combination of three weld-wire compositions, two tungsten arc-welding processes, and two heat-treating and welding sequences. The base material chosen for this study was vacuum-arc-remelted 12-5-3 maraging steel.

Three weld-wire compositions were chosen from the available wires to give the widest possible variation in titanium and nickel contents. The titanium content was of particular concern, since several investigators have found that fractures in maraging steel nucleate from titanium-nitride and titanium-carbide inclusions. (See Ref. 9.) Analyses of the three weld wires are given in Table 1 along with the analysis of the base plate. Weld wire from heat number 03028 was chosen as nearly matching the base-plate composition. Heat number 09794 contains a higher percentage of nickel, lower aluminum, and cobalt in place of chromium as is normal in the 18%-Ni alloy. This alloy is recommended by two steel companies for use in welding the 12%-Ni plate. Heat number 09847 differs from 09794 by having a still higher nickel content and significantly less titanium. These three wires are representative of what is commercially available for use in welding 12-5-3 material.

It is generally accepted that the tungsten-inert-gas process produces a highly acceptable multipass weld in thick plates of maraging steel. Of the welding processes that are presently commercially available, the TIG process generally produces the strongest and toughest joints in the maraging alloys. This has been confirmed by several studies (3, 4), so for this program other types of welding were not considered; only variations within the TIG process are used. One process, using standard 1/8-in.-diam tungsten electrode and the normal current, is referred to in this report as Standard TIG. Another process which makes use of a larger, 1/4-in.-diam, electrode with somewhat higher current is, for the purposes of this report, referred to as Big TIG.

The maraging steels can be welded in either the annealed or fully aged condition. Both sequences were entered into in this study to determine whether either offered any significant advantage. The plate material was received

from the mill in the solution-treated condition. The plates had actually been double annealed at the mill; 1650°F for one hour, water-quenched, 1500°F for one hour, and water-quenched again. Some panels were welded in this condition and then aged, while others were aged, welded, and then reaged. In each instance the age treatment was 900°F for 5 hours followed by cooling in air.

Twelve panels were welded using all possible combinations of the three wires, the two welding processes, and the two heat-treating and welding sequences. These panels were evaluated to determine tensile, impact, fracture-toughness, hardness, and metallurgical properties in an effort to find the optimum combination of parameters.

In practical application it seems highly probable that it will be necessary to make weld repairs. Defective welds, once located through nondestructive testing, could be removed and replaced with sound weld deposits. Such repairs might be required either before or after the structure's aging cycle, but in either case the new weld would require aging. (This aging could conceivably be local and would not necessitate reaging the entire structure.) To simulate such cases, panels were fabricated using the optimum parameters determined from the twelve panels previously evaluated. One of these panels was processed in each of the two heat-treating and welding sequences described above. Each panel was repaired three times, twice automatically and once by hand. These two repaired panels were then evaluated in the same way as were the twelve original panels.

## DATA AND TEST RESULTS

### Welded Test Panels

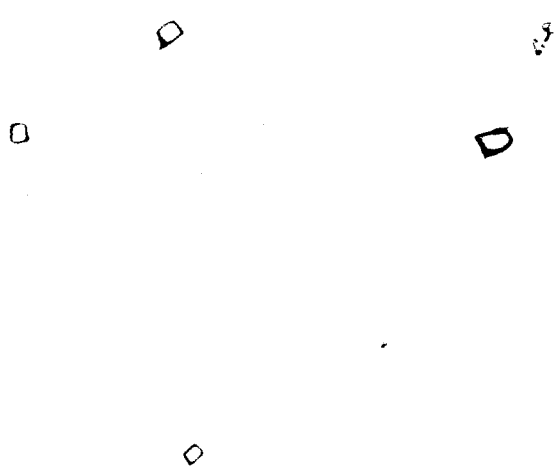
Samples from each of the three heats of weld wire were mounted in plastic and polished for metallographic examination. A comparison of the microstructures with ASTM Chart E-45-51 indicated good cleanliness for all three heats. Each heat was assigned a rating number of less than one for the standard sulfide, alumina, silicate, and globular oxide types of inclusions. When viewed under higher magnification (500X), small background inclusions were identified as titanium carbonitride and slag. Typical longitudinal sections near the center of the wire are shown in Fig. 4. The inclusion ratings were the same near the surface as in the interior of the wires. However, there was a noticeable difference in the surface finishes. The surface of the wire from heat 03028 was smooth compared with that of the other two wires. Figure 5 shows a comparison of the wire surfaces. Although the effect of surface roughness has not been established, the smooth condition is believed to be more desirable. The 09794 filler wire was 0.093 in. in diameter. The other two wires were 0.062 in. in diameter.

Twelve test panels were welded using all possible combinations of the three weld wires, two welding processes, and two heat-treating and welding sequences. These parameters were discussed in detail earlier in this report. Each panel was 11 by 20 in. and cut so that the final roll direction in the 1-1/8-in.-thick parent plate ran parallel to the 20-in. panel dimension. The panels were grooved, as shown in Fig. 6, and welded on the center line of the panel running parallel to the long dimension. All welding was horizontally positioned, preheated to 125°F, and welded by the heliarc process. Each aging cycle was at 900°F for 5 hours followed by air cooling.

In previous work with 18%-Ni maraging steel (4), the center of the weld was found to have the lowest fracture toughness. This was expected to also be the case for the 12-5-3 material. However, a few standard Charpy-V-notch impact specimens were notched in the center of the weld and a few in the heat-affected zone of the weld to determine which area was more brittle. Since this brittleness would result from the weld process or heat treating, there was no need to test all three weld compositions. The data presented in Table 2 indicate that the center of the weld is in fact slightly more brittle. It is the minimum fracture toughness that is of concern to the design engineers; therefore, the  $K_{Ic}$  measurements were made at the center line of the weld.

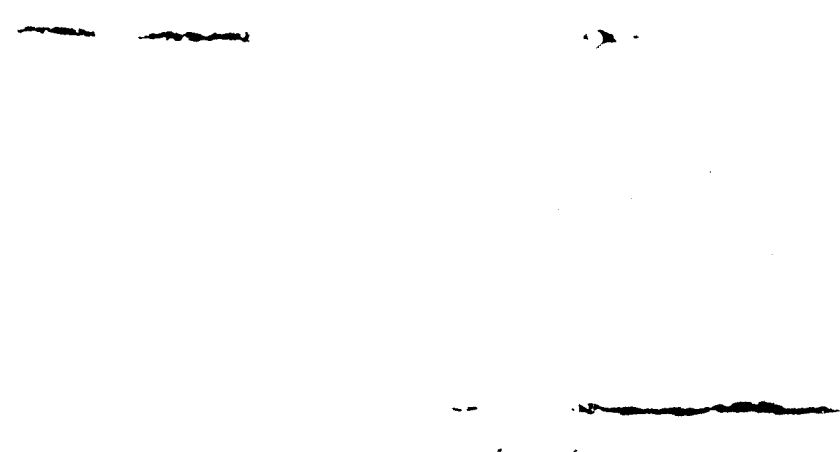
Tensile, Charpy-impact, fracture-toughness, and metallographic specimens were cut from each welded panel as shown in Fig. 7. The tensile data were obtained from the standard 0.505-in.-diam specimen. Standard Charpy-V-notch specimens were used in the impact tests. These were tested both as standard and as precracked specimens. The fracture-toughness specimens were the single-edge-cracked three-point bend bar as shown in Fig. 1. The bars were 1 by 1 by 10 in. with a 5% side groove on two sides and notched to a depth of 20%. The notch was extended by sinusoidal cyclic loading to a depth of approximately 30% of the specimen depth. The metallographic specimens were used in the hardness survey as well as the metallographic study.

STONESIFER AND SMITH



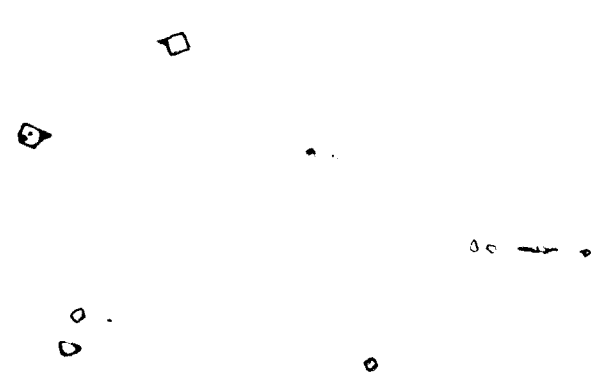
(a) Heat 03028, primarily titanium carbonitride inclusions (cubic particles)

This micrograph shows several small, dark, cubic-shaped particles scattered across the field of view. The particles are roughly equiaxed and have sharp edges. The background is a light, uniform color.



(b) Heat 09794, both slag (elongated particles) and carbonitride inclusions

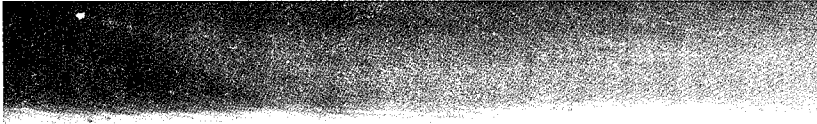
This micrograph displays a variety of inclusions. There are several dark, elongated, horizontal particles that appear to be slag. Interspersed among these are smaller, dark, cubic particles, which are identified as carbonitride inclusions. The distribution is somewhat irregular.



(c) Heat 09847, carbonitrides with a few slag inclusions

This micrograph shows a higher density of small, dark, cubic particles compared to (a). There are also a few larger, dark, elongated particles scattered throughout, representing slag inclusions. The overall appearance is more cluttered than in (a).

Fig. 4 – Typical longitudinal sections near center of wire (unetched, 500X).



(a) Heat 03028



(b) Heat 09794



(c) Heat 09847

Fig. 5 – Typical longitudinal sections at wire surface (unetched, 500X).

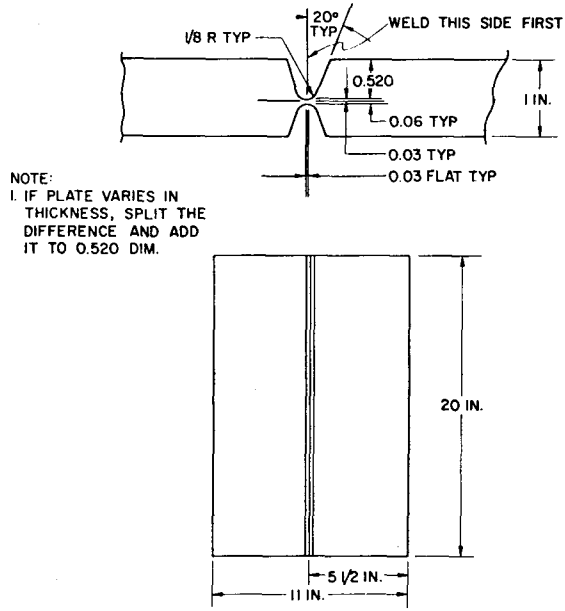
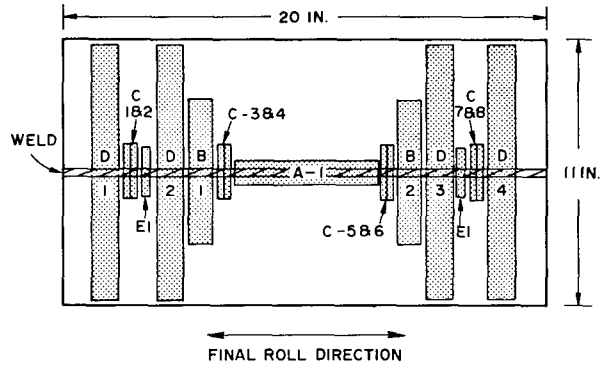


Fig. 6 – Weld preparation for test panels.



- A - "ALL WELD" TENSILE SPECIMEN
- B - TRANSVERSE TENSILE SPECIMENS
- C - CHARPY-V-NOTCH IMPACT SPECIMENS
- D - FRACTURE TOUGHNESS SPECIMENS
- E - METALLOGRAPHIC SPECIMENS

Fig. 7 – Specimen layout for welded test panels.

Table 2  
Charpy-V-Notch Data Used in Determination of Most Brittle Weld Area

Welding Process*	Heat-Treating Sequence	Notched in Heat-Affected Zone			Notched in Center of Weld		
		Energy† (ft-lb)	No. of Tests	Standard Deviation	Energy† (ft-lb)	No. of Tests	Standard Deviation
Big TIG	Solution-treated, welded, and aged	48.0	2	(2.0)	41.8	4	4.5
Std. TIG	Solution-treated, welded, and aged	54.5	4	2.1	45.0	4	3.6
Big TIG	Solution-treated, aged, welded, and reaged	52.0	2	(0)	50.5	4	1.7

\*All three panels were welded with 03028 wire.

†Standard Charpy-V-notch specimens were used.

Results of these tests are presented in the following tables and figures. Table 3 lists, for comparison, the base-plate properties. Properties and parameters for the twelve welded panels are given in Table 4. Figure 8 shows the etched section through two typical welds. No significant metallographic difference was apparent between welds produced by the two methods.

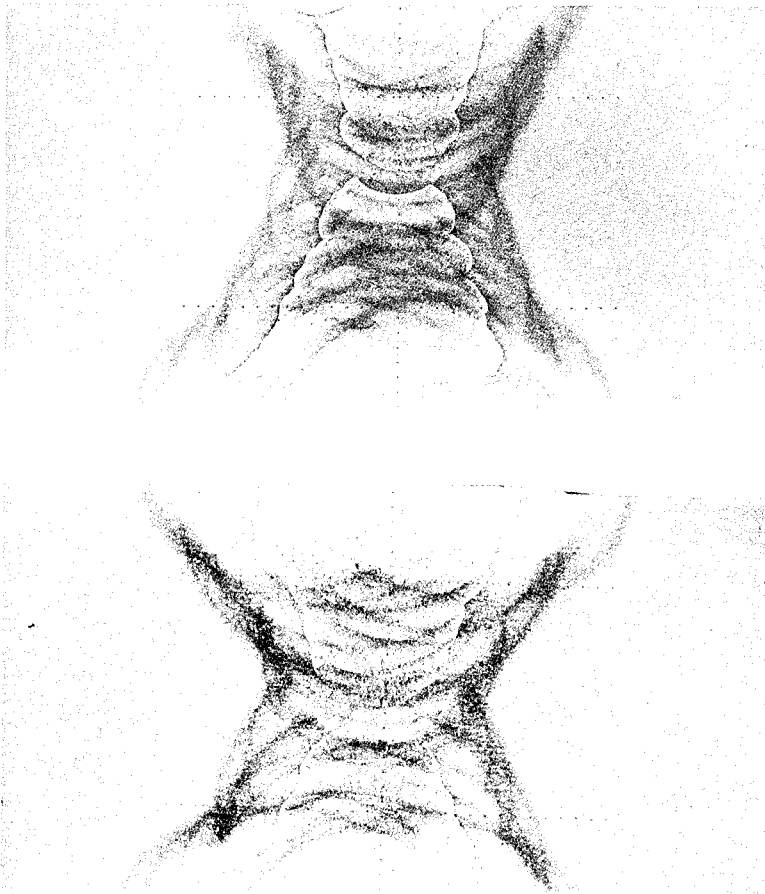


Fig. 8 – Typical sections through welds (2X, Wazau etch).

Table 3  
Properties of Aged Base Plate\*

Yield Strength	Ultimate Strength		Reduction in Area		Elongation, 2-in. gage		Young's Modulus		Standard Charpy Impact		Precracked Charpy		Apparent Fracture Toughness, Corrected†		Apparent Fracture Toughness, Uncorrected		Ratio, $K_{Ic}$ (corrected)/ $\sigma_y$										
	No. of Tests	Value (ksi)	Std. Dev. (ksi)	No. of Tests	Value (%)	Std. Dev. (%)	No. of Tests	Value (ft-lb)	Std. Dev. (ft-lb)	No. of Tests	Value (ft-lb/in. <sup>2</sup> )	Std. Dev. (ft-lb/in. <sup>2</sup> )	No. of Tests	Value (ksi $\sqrt{in.}$ )	Std. Dev. (ksi $\sqrt{in.}$ )	No. of Tests		Value (ksi $\sqrt{in.}$ )	Std. Dev. (ksi $\sqrt{in.}$ )								
Parallel to Final Roll Direction																											
3	183.8	3.3	3	189.6	3.3	3	57.4	1.8	3	14.1	0	3	26.6	1.3	4	102	5.2	4	700	73.1	10	202.7	5.8	10	170.0	5.8	1.10
Perpendicular to Final Roll Direction																											
4	174.5	0.5	4	186.2	3.2	4	84.8	2.8	4	13.9	0.3	4	29.2	0.7	4	68	5.9	4	450	52.4	9	253.4	21.4	9	185.9	6.4	1.45

\*Average hardness through thickness: 41, Rockwell C; 415, Vickers number.  
 †Corrected using the new scaling method based on equivalent elastic fracture strain.

Table 4  
Properties of Welded Panels

Filler-Wire Heat Number	Welding Current (A)	Welding EMF (V)	Tensile Properties										Standard Charpy Impact‡ (ft-lb)	Precracked Charpy Impact‡ (ft-lb/in. <sup>2</sup> )	Apparent $K_{Ic}$ (ksi $\sqrt{\text{in.}}$ )§		Ratio, $K_{Ic}$ (corrected to $\sigma_y$ (transverse))	Average Through-Thickness, Hardness at Weld Center (Vickers)
			Yield Strength (ksi)		Ultimate Strength (ksi)		Reduction in Area (%)		Elongation, 2-in. (%)		Young's Modulus ( $\times 10^{-6}$ )				Corrected	Uncorrected		
			Long.*	Trans.†	Long.	Trans.	Long.	Trans.	Long.	Trans.	Long.	Trans.						
Solution treated, welded, and aged. Welding process: Big TIG.																		
03028	220-260	11-12	190	187.4	199.5	194.3	38.5	51.7	10.9	10.9	26.8	27.7	41.8	208	134.9	131.3	0.72	449
09794	200-280	11	184.0	185.0	184.5	188.8	54.1	51.9	12.5	10.9	26.7	27.7	42.8	260	161.8	144.4	0.87	426
09847	200-260	10-12	188.5	188.0	194.0	192.0	55.0	55.4	14.1	11.3	27.6	26.9	51.3	309	182.5	161.1	0.97	435
Solution treated, welded, and aged. Welding process: Standard TIG.																		
03028	125-225	11	185.5	186.0	192.0	191.0	58.5	41.9	14.1	11.8	27.7	26.7	45.0	276	241.9	194.7	1.30	441
09794	190-240	10-11	179.0	183.7	186.1	186.0	54.0	21.1	13.3	4.7	27.7	27.1	55.8	277	182.4	155.8	0.99	427
09847	180-220	10-11	180.6	186.4	185.3	191.7	62.7	58.6	13.3	12.5	26.5	26.8	39.3	400	193.3	168.4	1.04	428
Solution treated, aged, welded, and reaged. Welding process: Big TIG.																		
03028	210-250	10-12	187.0	185.3	194.0	192.1	53.5	52.8	11.7	11.3	28.6	27.2	50.5	202	199.6	171.1	1.08	432
09794	170-250	10-12	180.8	185.5	188.5	189.3	58.5	52.2	11.7	10.2	27.3	27.2	43.8	245	184.7	151.5	1.00	410
09847	210-250	10-12	182.3	188.0	187.9	192.5	55.1	53.5	13.3	10.9	25.9	26.8	30.5	421	219.9	188.1	1.17	428
Solution treated, aged, welded, and reaged. Welding process: Standard TIG.																		
03028	125-220	11	185.0	186.2	193.5	189.7	58.0	53.7	13.3	11.8	26.9	26.9	37.0	301	216.1	183.3	1.16	439
09794	170-235	10-11	182.8	184.0	190.1	186.7	54.2	16.2	14.1	7.0	27.3	27.5	48.5	252	227.8	183.1	1.24	410
09847	175-235	10-11	184.5	188.5	190.0	192.7	56.5	57.9	11.7	11.7	28.0	27.8	46.8	385	236.1	187.8	1.25	441

\*Longitudinal (all weld material).

†Transverse (across the weld).

‡Notched on weld center.

§Corrected using the new scaling method.

Vicker's diamond pyramid hardness readings were taken at 1-mm intervals along the weld center line in the through-the-thickness direction. Two hardness surveys were also run across the weld, one at 1/4 in. from each of the plate surfaces. These data are plotted as hardness profiles in Fig. 9 through 12. In general, the weld deposit is harder than the base plate, whereas the heat-affected zone is softer. This would tend to substantiate the data shown previously in Table 2.

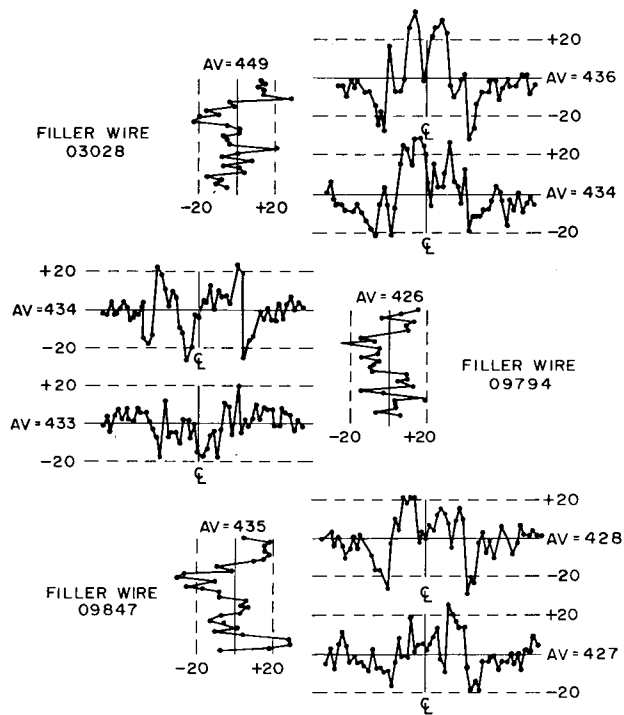


Fig. 9 – Hardness profiles of welds; Vickers hardness number, 20-kg load, readings 1 mm apart. Specimens solution treated, welded, and aged; Big TIG.

The metallographic examination was concentrated at the quarter-point thickness, midway between center and surface of the plate. This location represented an average condition and was near the depth at which fracture toughness was measured.

The base plate steel had a low inclusion content, as is typical of the vacuum-melted materials. Fig. 13a shows a typical field where the larger particles were identified as titanium carbonitrides and the smaller inclusions were chiefly globular-type oxides. The inclusion rating was less than 1 on the ASTM chart, indicating a high degree of cleanliness. The grain size was fine, about 5 on the ASTM chart, and nearly uniform from the center to the plate surface. Figure 13b illustrates the fine grain size while the expected martensitic structure may be better observed in Fig. 13c at a higher magnification. Only a weak banding pattern was present, indicating a minimum of segregation.

Microscopic inspection revealed no important differences between the two welding processes, the three weld wires, or the two heat-treating sequences. The deposited weld metal was clean except for an occasional rounded inclusion.

The weld metal had a coarse dendritic structure which, except for the outer passes, had been refined to a smaller grain size by the heat of subsequent passes. The outermost beads could have been refined also by applying

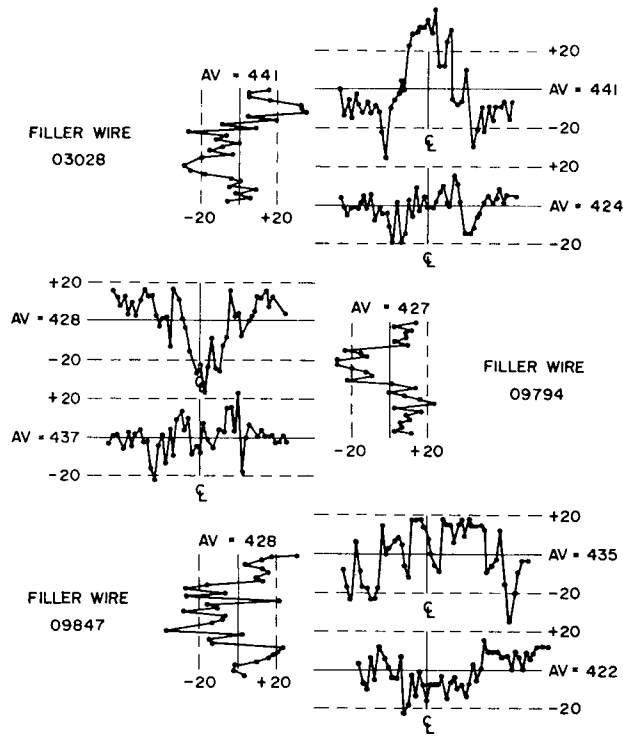


Fig. 10 – Hardness profiles of welds; Vickers hardness number, 20-kg load, readings 1 mm apart. Specimens solution treated, welded, and aged; Standard TIG.

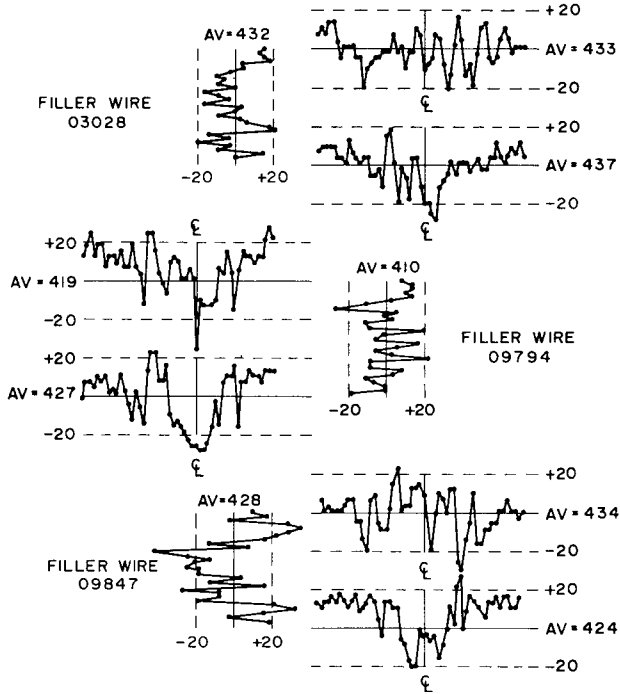


Fig. 11 – Hardness profiles of welds; Vickers hardness number, 20-kg load, readings 1 mm apart. Specimens solution treated, aged, welded, and reaged; Big TIG.

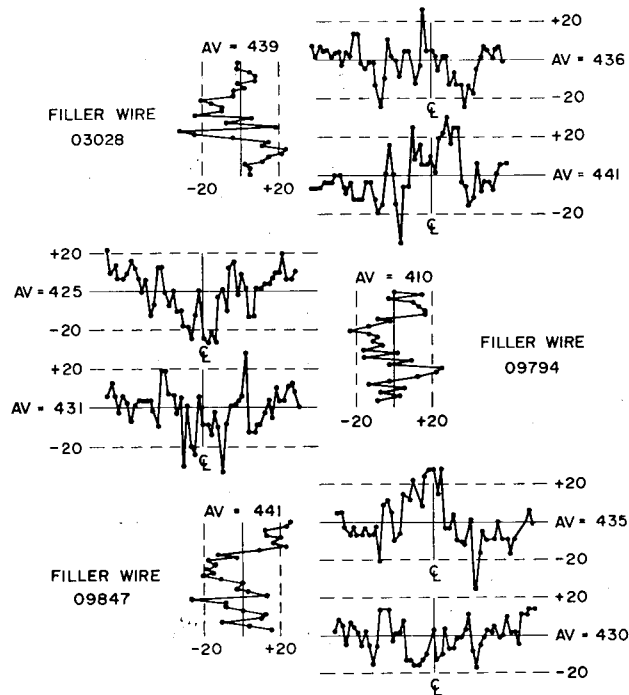


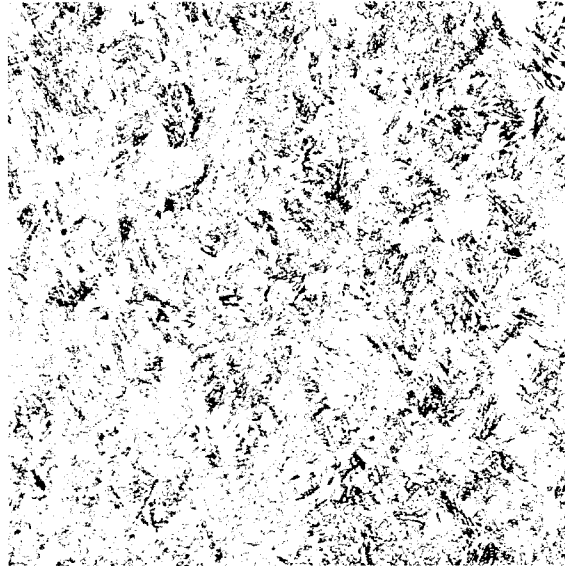
Fig. 12 — Hardness profiles of welds; Vickers hardness number, 20-kg load, readings 1 mm apart. Specimens solution treated, aged, welded, and reaged; Standard TIG.

an extra buildup which could then be ground off. There was no visible evidence of austenite cores in the dendritic pattern, as shown in Fig. 14. A general inspection of the sample areas did not reveal any microcracks. The dark network pattern results from dendritic segregation during solidification. The absence of visible white cores in the dark spots implies that retained austenite, if present, is in small amounts. The lighter basket-weave structure indicates grain size refinement by heat of subsequent weld passes. Among the various welds, no significant difference was noted that could be attributed to the varied parameters.

The purpose of this study as previously mentioned, was to determine which combination of parameters would produce the optimum weld. For the proposed applications, we are predominately interested in fracture toughness, and yield strength, and their ratio to each other. There are various ways of comparing and evaluating the test data. One way of comparing the results is shown in Table 5, where one parameter is considered at a time and all the data associated with it are averaged for comparison. From such a comparison we see that the low-titanium alloy, wire 09847, seems to offer a slight advantage over the other two wires. Aging the plate before as well as after welding tends toward a tougher weld; however, in some cases the additional cost may not be justifiable. The so-called Big TIG welding process offers a slight advantage in strength. However, this is more than canceled by the loss in toughness. From this information it was decided that the panels to be used in the weld repair experiment should be welded by the standard TIG process using weld wire from heat 09847.

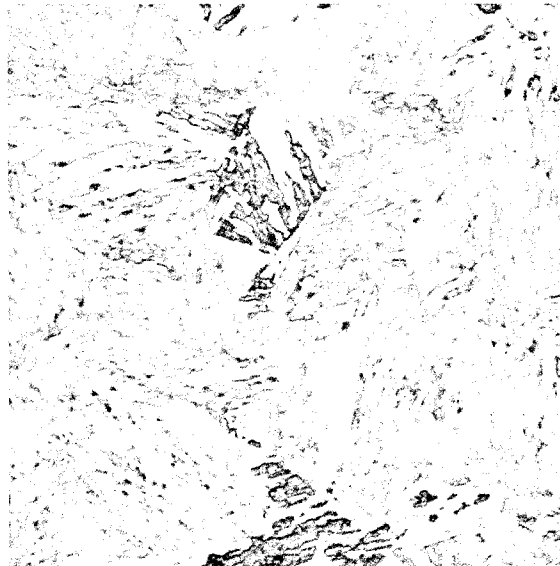
### Weld Repairs

The last two panels were welded and repaired using these optimum parameters. After the initial welding, a V-groove was ground into one side of the weld to a depth of half the plate thickness. The groove ran the full length of the panel and removed 40 to 60% of the original weld metal deposited on that side of the plate. The groove was then filled in again with weld. The process was repeated three times to simulate multiple repairs which might become necessary in field applications. The repairs were made automatically twice, but the third and final repair was made manually. One panel was heat treated in accordance with each of the two previously described sequences. The



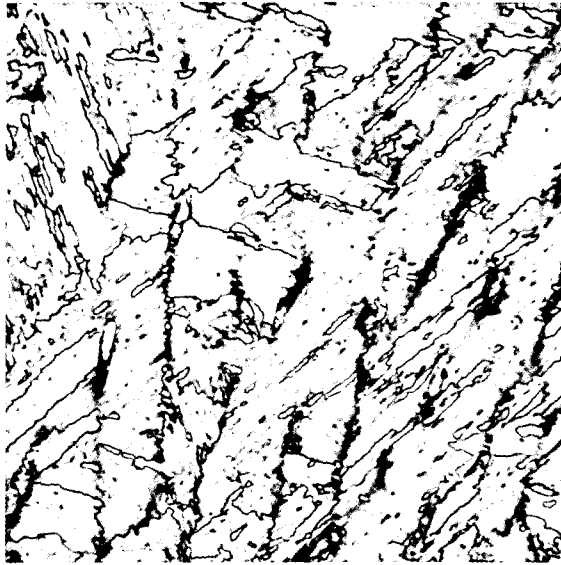
(a) Typical inclusions (unetched, 100X)

(b) Grain Structure rated approximately 5 on the ASTM scale (Wazau etch, 100X)

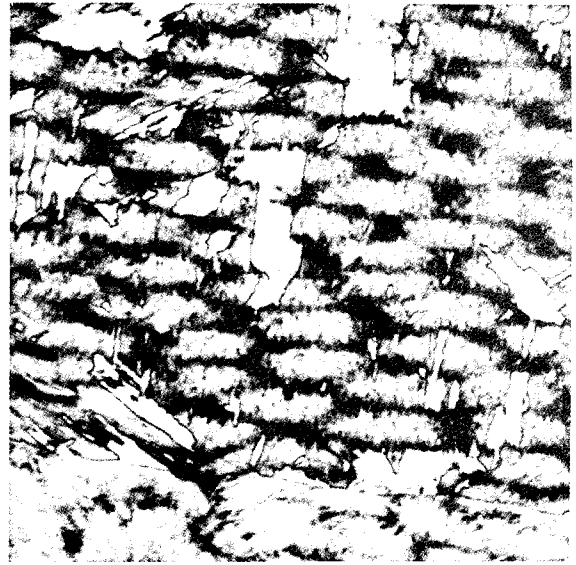


(c) The martensitic grains are more distinct at a higher magnification (Wazau etch, 500X)

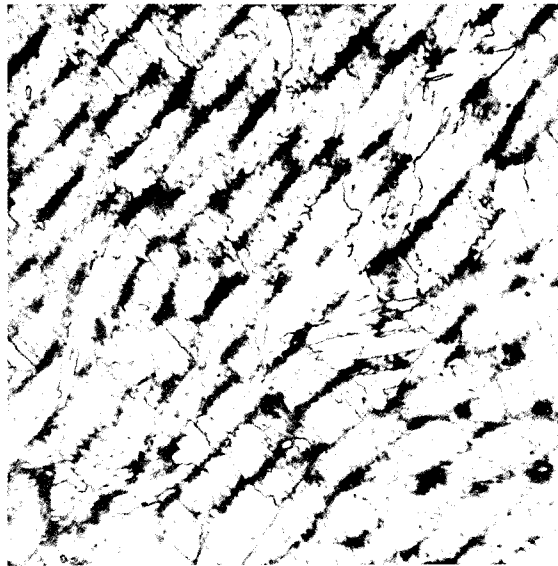
Fig. 13 – Microstructure of base plate.



(a) Big TIG weld, 09794 wire, solution treated, welded, and aged (Wazau etch, 500X)



(b) Standard TIG, 09847 wire, solution treated, welded, and aged (Wazau etch, 500X)



(c) Big TIG weld, 03028 wire, solution treated, aged, welded, and reaged (Wazau etch, 500X)

Fig. 14 – Typical microstructures of weld.

Table 5  
Comparison of Parameters

Parameter	Avg $\sigma_y$ (ksi)	Avg $K_{Ic}$ (Cor.) (ksi $\sqrt{\text{in.}}$ )	Avg $K_{Ic}/\sigma_y$
Welded with 09794 wire (recommended by vendors)	184.6	189.2	1.03
Welded with 09847 wire (low titanium, 0.19%)*	187.7	208.0	1.11
Welded with 03028 wire (nearly matching the base plate composition)	186.2	198.1	1.07
Solution treated, welded, and aged (aged 5 hr at 900°F)	186.1	182.8	0.98
Solution treated, aged, welded, and reaged (aged 5 hr at 900°F)*	186.3	214.0	1.15
Big TIG (200-260 A at 10-12 V)	186.5	180.6	0.97
Standard TIG (170-235 A at 10-11 V)*	185.8	216.3	1.16

\*These were considered the optimum processes.

panels were cut into specimens as illustrated earlier in Fig. 7. The properties as obtained from these tests are presented in Table 6. One may note from a comparison between the data from the repaired panel and that from the similar straight weld panel that the corrected fracture toughness  $K_{Ic}$  has been reduced by 25.6% in the case of the aged and reaged panel but only by 7.1% for the aged panel. The yield strength has increased by an insignificant 4.3 and 2.4% for the aged and reaged panels, respectively.

Hardness surveys of the multiple welds in the repaired panels are shown in Fig. 15. These multiple welds might have been expected to show more heat effects than regular welds. A "white" etch-resistant film about 0.01-in. thick at the weld fusion line (see Fig. 16a) showed a drop in hardness of about 10% because of poor response to aging. This layer probably was remelted base metal. The dark-etched bands out in the so-called eyebrow region where the peak temperature reached approximately 1200°F had a local lowering in hardness of about 5% because of partial reversion to stable austenite. There seemed to be nothing unusual in the soft zones as compared to the regular welds; minor differences would have been difficult to evaluate. Such small zones of localized hardness deficiency commonly are associated with maraging steel welds and usually have no serious effect on overall strength properties.

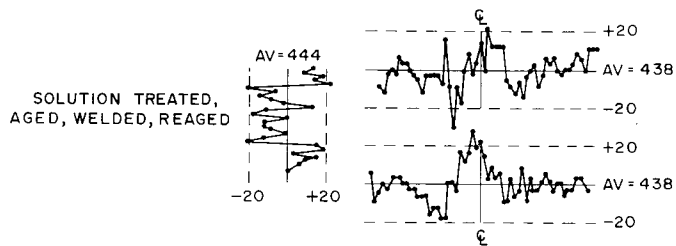


Fig. 15 - Hardness profiles of repair welds; Vickers hardness number, 20-kg load, readings 1 mm apart, welded with filler wire 09847; Standard TIG.

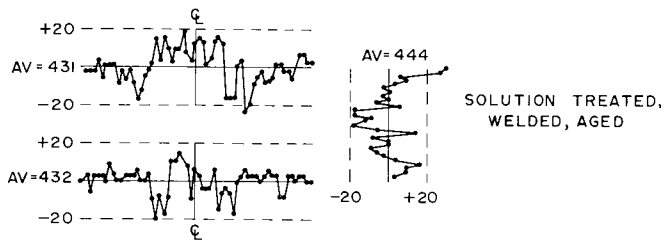


Table 6  
Properties of Repaired Welded Panels

Filler-Wire Heat Number	Automatic Repair		Manual Repair		Tensile Properties								Standard Charpy Impact ‡ (ft-lb)	Precracked Charpy Impact ‡ (ft-lb/in.2)	Apparent $K_{Ic}$ (ksi $\sqrt{\text{in.}}$ ) §		Ratio, $K_{Ic}$ (corrected) to $\sigma_y$ (transverse)	Average Through-Thickness Hardness at Weld Center (Vickers)		
	Welding Current (A)	Welding EMF (V)	Welding Current (A)	Welding EMF (V)	Yield Strength (ksi)		Ultimate Strength (ksi)		Reduction in Area (%)		Elongation, 2-in. (%)				Young's Modulus (X10 <sup>-6</sup> )				Corrected	Uncorrected
					Long.*	Trans.†	Long.	Trans.	Long.	Trans.	Long.	Trans.			Long.	Trans.				
Solution treated, aged, welded, and reaged.																Welding process: Standard TIG.				
09847	200	12	175	10	189.0	193.3	196.5	198.3	56.0	53.4	12.0	11.5	25.9	27.5	45.8	32.8	175.6	156.3	0.91	441
Solution treated, welded, and aged.																Welding process: Standard TIG.				
09847	200	12	175	10	188.3	189.8	196.4	193.8	58.9	58.1	13.3	11.7	27.2	26.2	46.0	30.6	158.5	179.6	0.95	441

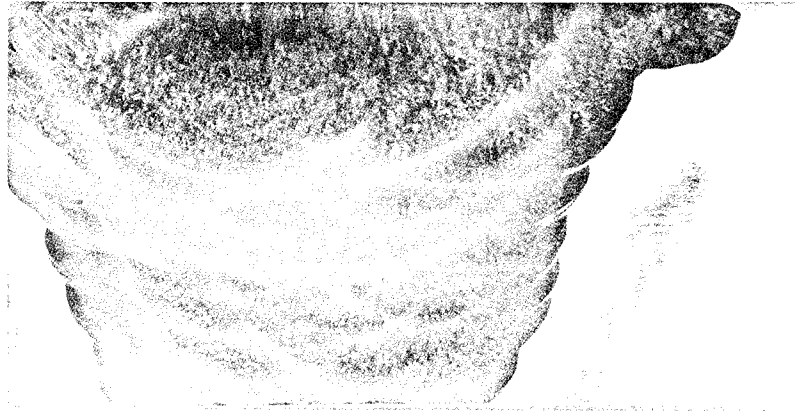
\* Longitudinal (all weld material).

† Transverse (across the weld).

‡ Notched on weld center.

§ Corrected using the new scaling method.

(a) Section through half of repaired weld. A distinction between the original and repair welds can be seen on the left side (mounted in plastic, Wazau etch, 4X)



(b) Weld metal in repaired weld with dendritic grain size of about 3 (Wazau etch, 100X)

(c) HAZ in parent metal adjacent to weld fusion line with grain size of about 4 (Wazau etch, 100X)

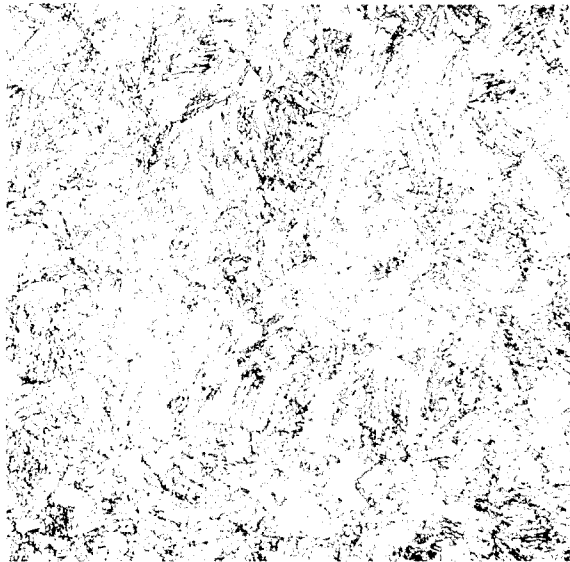


Fig. 16 – Microstructure of repaired weld.



The new scaling method for plasticity corrections was used and found to be superior to previous plasticity corrections. This new correction is not limited by the requirement that  $K_{Ic}^2/6\pi\sigma_y^2 \ll a_0$ , the crack depth, since it is based on an equivalent elastic-fracture strain rather than stress.

#### ACKNOWLEDGMENT

The authors are indebted to H. E. Romine and R. G. Hayes of the Naval Weapons Laboratory, Dahlgren, Virginia. Dr. Romine was responsible for the metallurgical study and micrographs. Mr. Hayes assisted in specimen preparation and hardness determinations. These tasks were performed at NWL for NRL under Contract WR-5-0057.

#### REFERENCES

1. Saperstein, S. P., and Mixon, W. V., "Evaluation of Maraging Steel for Application to Space Launch Vehicles, Contract NAS7-214 W00-PR-60-174, Final Report," Douglas Report SM-43105, Feb. 1964
2. Stonesifer, F. R., and Smith, H. L., "Fracture Toughness Measurements on 12%-Ni Maraging Steel Weldment," *Hydro-nautics*, Vol. 3 (No. 1); 54-57 (1969)
3. Tiffany, C. F., Masters, J. N., and Regon, R. E., "A Study of Weldments and Pressure Vessels Made of 12 Ni Maraging Steel," The Boeing Company, Contract P.O. 54-01109-21. Aerospace Group, Seattle, Wash.
4. Kies, J. A., Smith, H. L., Romine, H. E., and Bernstein, H., "Fracture Testing of Weldments," ASTM Symposium on Fracture Toughness Testing and Its Applications, Special Technical Publication, No. 381, 1965; also NASA Contractor Report, NASA CR-140, Dec. 1964
5. Stonesifer, F. R., "Fracture Toughness Equations for Bend Specimens," Report of NRL Progress, Feb. 1968, pp. 12-13
6. "Proposed Recommended Practice for Plane-Strain Fracture Toughness Testing of High-Strength Metallic Materials Using a Fatigue-Cracked Bend Specimen," ASTM Standards, 1968, Part 31, pp. 1018-1030
7. Kies, J. A., Smith, H. L., and Stonesifer, F. R., "Graphical Methods for Plasticity Corrections in Fracture Mechanics," NRL Report 6918, Sept. 18, 1969
8. Tetelman, A. S., and McEvily, A. J., Jr., "Fracture of Structural Materials," New York; Wiley 1967
9. Tobias, J. B., and Bhat, G. K., "Correlation of Weld Microstructure with Fracture Toughness of 18% Nickel (250) Grade Maraging Steel," prepared for Naval Research Laboratory under Contract Nonr-4595 (00) (X) by the Mellon Institute, Pittsburgh, Pa., Feb. 28, 1965

